



Citation for published version:

Siddiq, K, Hobden, MK, Pennock, SR & Watson, RJ 2018, 'Phase Noise in FMCW Radar Systems', IEEE Transactions on Aerospace and Electronic Systems. <https://doi.org/10.1109/TAES.2018.2847999>

DOI:

[10.1109/TAES.2018.2847999](https://doi.org/10.1109/TAES.2018.2847999)

Publication date:

2018

Document Version

Peer reviewed version

[Link to publication](#)

© 2018 IEEE. Personal use of this material is permitted. Permission from IEEE must be obtained for all other users, including reprinting/ republishing this material for advertising or promotional purposes, creating new collective works for resale or redistribution to servers or lists, or reuse of any copyrighted components of this work in other works.

University of Bath

General rights

Copyright and moral rights for the publications made accessible in the public portal are retained by the authors and/or other copyright owners and it is a condition of accessing publications that users recognise and abide by the legal requirements associated with these rights.

Take down policy

If you believe that this document breaches copyright please contact us providing details, and we will remove access to the work immediately and investigate your claim.

Phase Noise in FMCW Radar Systems

Kashif Siddiq, *CEng MIET*, Mervyn K. Hobden, *Hon. Fellow, BHI*, Steve R. Pennock, *Member, IEEE*,
and Robert J. Watson, *Member, IEEE*.

Abstract—Phase noise is one of the fundamental performance parameters in modern radar, communication, spectroscopic, and metrological systems. In this paper a phase noise theory has been developed for FMCW radar systems. A new design equation has been derived to specify the maximum bound on the allowable source phase noise level in radar systems. The non-linear phase noise decorrelation function due to coherent mixing has been analysed for propagation delays less than the coherence time of the reference oscillator, and the spectral broadening of target responses has been discussed for delay times greater than the coherence time. The effects of the subsystems in the transceiver chain are presented and a new model of phase noise in ADCs is discussed. Phase noise modelling techniques are presented, followed by a comparison of a PLL frequency synthesiser with a low-noise frequency synthesiser to demonstrate the reduction of phase noise sidebands for improved detection and tracking performance. Practical measurements from two millimetre wave FMCW radar systems utilising the two frequency synthesisers have been presented to validate the developed theory.

Index Terms—Phase noise, FMCW radars, coherence, spectral analysis, phase noise cancellation.

I. INTRODUCTION

A perfect monochromatic sinewave is an idealisation available only in textbooks. All natural and man-made oscillators (whether optical, electronic, acoustic, atomic, or any other) exhibit phase and frequency instabilities collectively known as *Phase Noise*. These instabilities are related to the materials making up the oscillator, the architectural design of the oscillator, and the random noise phenomena in the oscillator. This paper deals with the analysis of phase and frequency instabilities in the oscillators used in frequency modulated continuous wave (FMCW) radar systems.

It is well-known that the short-term frequency instability in oscillators, described by the phase noise, manifests itself as phase modulation sidebands in oscillator spectra [1]–[3]. Linear phase noise analysis [4]–[8] deals with the analysis of the low-noise sidebands only in the RF spectrum of an oscillator [4], [5], [9]. However the phase noise processes also give rise to a nonlinear near-carrier spectrum [10]–[13], a phase noise *floor*, and broadening of the linewidth of the oscillator signal’s RF spectrum [12], [14], [15]. A complete phase noise analysis must include all portions of the RF spectrum.

Excessive phase noise in an oscillator (greater than 1 rad^2) leads to severe distortion in the RF spectrum in the form

Manuscript received March xx, 2017. Revised August xx, 2017 This work was partially supported by Innovate UK. The radar sensors for this work were supplied by Navtech Radar Ltd.

Authors’ Addresses: K. Siddiq, R. J. Watson, S. R. Pennock, Department of Electronic and Electrical Engineering, University of Bath, Claverton, Bath, BA2 7AY UK. E-mail: (kashif.siddiq@bath.edu).

M. K. Hobden, Navtech Radar Ltd., Home Farm, Ardington, Wantage, OX120PT, UK. E-mail: (merv.hobden@navtechradar.com).

of a widened central peak and distorted sidebands. A well-designed coherent radar system should have an integrated phase noise much less than 1 rad^2 . In this paper an analysis will be presented as the phase noise in a signal approaches this limit under frequency multiplication and new results will be presented for the allowable noise-sideband level in the transmitted signal to comply with this limit. The noise sideband response produced by radar systems is a function of the target’s range (i.e. time delay) [4] and even if a low-phase noise master oscillator is employed in a radar, the demodulated return signal loses *coherence* with the transmitted signal due to the frequency drift processes present in the oscillator. Therefore, a well-designed radar should operate well within the *coherence time* of the oscillator [14], [16] to avoid excessive broadening of the demodulated signal’s spectrum.

Phase noise in FMCW radars has not received a detailed attention as in other areas of radar systems. The present paper attempts to fill in this void. In particular, this paper considers the effects which are significant for compact low-cost radars, which now constitute an important field of application of FMCW radar systems. From the systems aspect, phase noise in FMCW radars has been addressed from various aspects in [5], [17]–[22]. In [5] the fundamentals of FMCW system design have been presented including some noise aspects. In [17] the impact of coherent integration on phase noise has been addressed. In [18] the impact of oscillator noise parameters like the noise figure and the corner frequency on the phase noise performance has been analysed. In [5] and [19] the impact of the internal noise leakage through the receiver’s mixer has been analysed in detail. In [20]–[22] some post-processing phase noise reduction techniques have been proposed.

An important aspect of the present work is the demonstration of how to accurately relate the source phase noise to the phase noise in the IF signal’s spectrum by quantifying the phase noise introduced by the various stage of a typical FMCW radar system, and the demonstration of the reduction in phase noise by utilising a properly designed radar signal source. Using those guidelines one can work back to determine the source phase noise level required to achieve a given specification of the dynamic range.

The rest of this paper is organised as follows. Section II presents the fundamentals of phase noise including the notation and the definitions used in the paper. The development of the phase noise models of the radar subsystems is presented in Section III to present a phase noise modelling methodology for FMCW radar systems. New results on phase jitter cancellation in analog-to-digital converters are presented. In section IV, the derivation of a novel design equation is presented to prevent excessive demodulated phase noise due

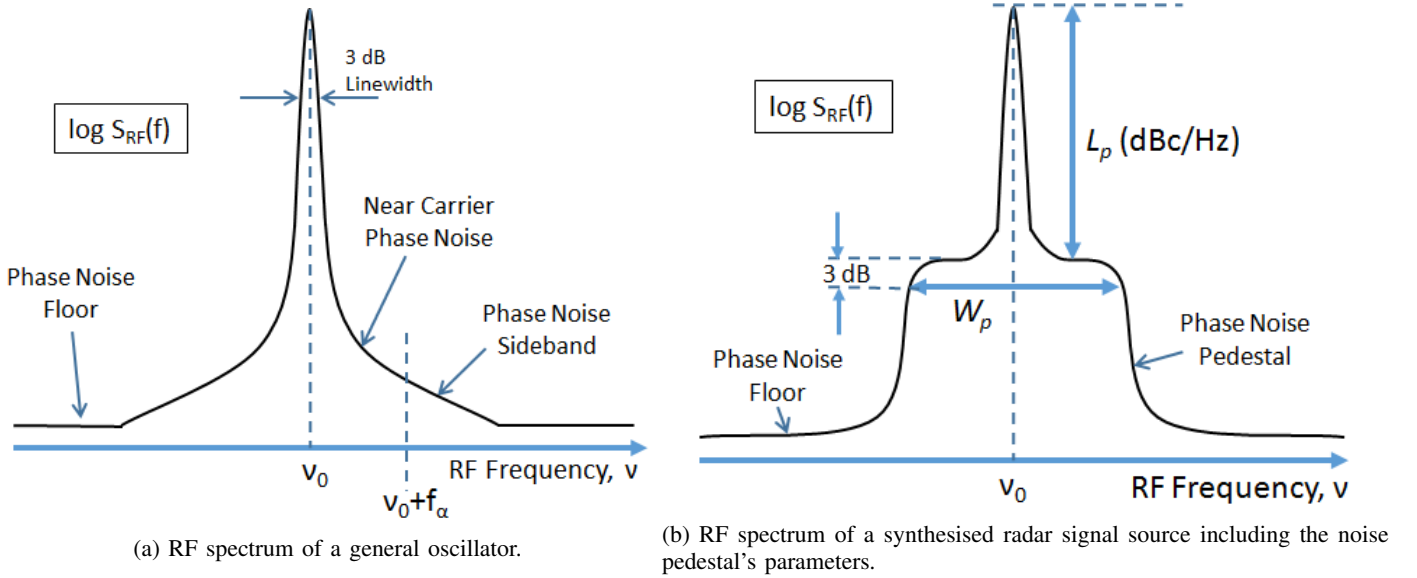


Fig. 1: Illustration of the RF spectra of radar signal sources.

to the source phase noise and/or frequency multiplication in the transmitter. Section V demonstrates the application of the modelling methodology for the accurate modelling of phase noise in a practical millimetre wave (MMW) radar system. The benefits of using a low-phase noise frequency synthesiser to achieve high dynamic range target discrimination will be demonstrated using practical measurements.

II. CHARACTERISATION OF PHASE NOISE IN RF SPECTRA

Phase noise in oscillators is most popularly characterised by the *spectral density of phase fluctuations* $S_\phi(f)$ that normally consist of power law frequency components [23]. On the other hand, practical radio, radar, and spectroscopic systems, to name a few, use the RF spectrum of the oscillator $S_{RF}(\nu_0, f)$ as the *working* spectrum during their operation, and will be the focus in the forthcoming discussion. Fig. 1a illustrates the RF spectrum $S_{RF}(\nu_0, f)$ of a general oscillator, where ν_0 is the centre- or carrier-frequency of the measured spectrum, and f is the *offset frequency* from the carrier frequency. When the sidebands in $S_{RF}(\nu_0, f)$ are due to phase modulation (PM) noise, they are referred to as *Phase noise* sidebands, are denoted by $\mathcal{L}(f) = S_{RF}(\nu_0, f)/P$ (where P is the total power in the measured oscillator signal), and have the units of decibels relative to the carrier per Hertz (dBc/Hz).

As shown in Fig. 1a the frequency offset $f = f_\alpha$ divides the phase noise portion of the spectrum into two part, i.e., the near-carrier phase noise and the far-from-carrier phase noise. The IEEE Standard 1139-1999 [23] defines phase noise as,

$$\mathcal{L}(f) = \frac{S_\phi(f)}{2}. \quad (1)$$

$\mathcal{L}(f)$ in this definition is a single-sided quantity, and is related to $S_{RF}(\nu_0, f)$ only in the far-from-carrier region, i.e., for all $f \geq f_\alpha$ such that,

$$\int_{f_\alpha}^{\infty} S_\phi(f) df = 0.1 \text{ rad}^2. \quad (2)$$

Below f_α , $S_{RF}(\nu_0, f)$ is nonlinearly related to $S_\phi(f)$. A nonlinear relationship between $S_\phi(f)$ and the normalised two-sided baseband RF spectrum $S_{RF}^b(f)$ is given in [10]–[12] as,

$$S_{RF}^b(f) = e^{-\sigma_\phi^2} \left[\delta(f) + S_\phi(f) + \frac{1}{2!} S_\phi(f) * S_\phi(f) + \dots \right], \quad (3)$$

where σ_ϕ^2 is the variance of the phase noise process $\phi(t)$, or equivalently,

$$\sigma_\phi^2 = \int_0^{\infty} S_\phi(f) df, \quad (4)$$

and is assumed to be finite. Equation (3) can be used to model the near-carrier phase noise as well as the far-from-carrier phase noise, although in the latter case (1) is easier to use. In (3) the carrier has been modelled as a Delta function: in practice $S_{RF}(f)$ has a finite linewidth and a defined lineshape that are a function of the frequency noise processes in the oscillator. These are dealt with in [12], [14].

Fig. 1b illustrates a typical target spectrum displayed by a radar system employing a synthesised signal source. The phase noise *pedestal* can originate due to a phase locked loop (PLL) based synthesiser having a finite *loop bandwidth*, or due to the finite bandwidth of the frequency multiplier chain being employed in the system to frequency multiply, say, a crystal reference oscillator to higher frequencies. A detailed analysis of the behaviour of the noise pedestal under frequency multiplication can be found in [12], [24], [25] where measurements of the noise sidebands have been presented.

Equation (3) can also be written as,

$$S_{RF}^b(f) = S_{RF}^c(f) + S_{RF}^p(f), \quad (5)$$

where $S_{RF}^c(f)$ is the RF spectral density of the central carrier peak and $S_{RF}^p(f)$ is the RF spectral density of the phase noise pedestal. For linear phase noise analysis one has to invoke the low-phase noise condition, $\sigma_\phi^2 \ll 1$. Under this condition (3) simplifies to:

$$S_{RF}^b(f) \approx e^{-\sigma_\phi^2} [\delta(f) + S_\phi(f)]. \quad (6)$$

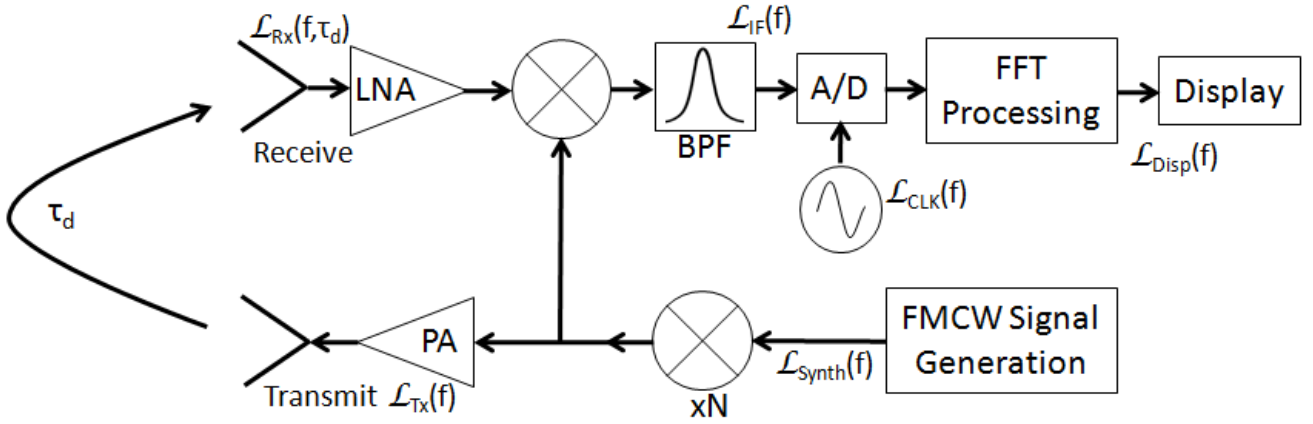


Fig. 2: Block diagram of a general FMCW radar system. The phase noise $\mathcal{L}(f)$ at various points in the system is marked.

The phase noise pedestal shown in Fig. 1b can be modelled by a modified Lorentzian function as follows:

$$S_{RF}^p(f) = \frac{2L_p}{1 + \left(\frac{|f|}{0.5W_p}\right)^k}, \quad (7)$$

where $S_{RF}^p(f)$ is the double-sided RF spectral density of the noise pedestal, L_p is the flat-top level of the pedestal (in dB-rad²/Hz), W_p is the 3-dB width of the noise pedestal, and k is the order of the roll-off and is generally between 2 and 4 for microwave frequencies. Under the low-phase noise condition, σ_ϕ^2 can also be computed from $S_{RF}^p(f)$ as,

$$\sigma_\phi^2 = \int_0^\infty S_{RF}^p(f) df. \quad (8)$$

In practice, the computation of this integral can be done for a finite upper limit of f defined by the width of the noise pedestal and the order of the roll-off. Also, the assumption of finite σ_ϕ^2 in (3) is only valid for a finite observation time T_{obs} (or measurement time) for the oscillator signal [6], [26]–[28], which in fact is equivalent to defining a non-zero low-frequency cutoff at $1/T_{obs}$ for the phase noise spectrum [27]. For excessively large measurement times, the flicker frequency and random-walk frequency components of phase noise cause excessive broadening of the measured RF spectrum [27]–[30].

Phase noise can be equivalently defined by the *timing jitter* in oscillators. The *RMS timing jitter* σ_t in a signal having a nominal radian operating frequency of $\omega_0 = 2\pi\nu_0$ is related to σ_ϕ^2 as [31],

$$\sigma_t = \omega_0 \sigma_\phi. \quad (9)$$

The timing jitter formulation of phase noise is especially helpful when analysing phase noise in ADCs.

III. PHASE NOISE IN THE ELECTRONIC SUBSYSTEMS

Fig. 2 shows a block diagram of the system under consideration which is a basic homodyne FMCW radar system. The *FMCW Signal Generation* block synthesises the FMCW waveform which is frequency multiplied up to the transmit frequency band using the $\times N$ frequency multiplier. The received signal is frequency mixed with the transmitted signal to generate the intermediate frequency (IF) signal: the frequency

difference between the transmitted signal and the received signal is proportional to the target's range [5]. The IF signal is digitised using an analog-to-digital converter (ADC or A/D). Complex Fast Fourier Transform (FFT) processing is then used to extract the information about targets like range, phase, signal strength, etc. In the following subsections, the phase noise contribution of these electronic subsystems is discussed.

A. Frequency Synthesisers

Indirect and direct frequency synthesisers [31]–[33] are used to generate the desired transmit waveform in radar systems. Popular examples include arbitrary waveform generators, Phase Lock Loops (PLL), Direct Digital Synthesisers (DDS), and variants based on these.

In PLL based frequency synthesis it is well-known that inside the loop filter's bandwidth, the reference oscillator's phase noise dominates, while outside the loop bandwidth the voltage controlled oscillator's (VCO) phase noise dominates [31]. Modern phase-frequency detector (PFD) based PLL's are versatile in that they perform automatic phase and frequency locking [31]. However for high dynamic range radar applications the phase noise performance of PFDs may not be acceptable [9] leading to high levels of in-band phase noise. The PLL-synthesised signal has a spectrum of the type shown in Fig. 1b which shows a noise pedestal around the carrier frequency.

To reduce the noise pedestal one solution is to reduce the loop bandwidth of the PLL. However that also reduces the modulation bandwidth of the system in the Type-2 PLL scheme [31] commonly employed. In the case of FMCW radars this is the bandwidth required to correctly synthesise the ramping waveform: excessive reduction of the loop bandwidth caused ringing in the transient response of the PLL. Therefore, the modulation requirement sets the limit on the least achievable loop bandwidth. PLL synthesisers have been discussed in [34]–[36] in the context of FMCW radar systems. Insufficient loop bandwidth can also cause the loop to become unlocked, especially if a fast flyback is required at the end of the sweep.

Offset PLLs [37]–[39] have been used successfully to improve the phase noise performance over conventional PLLs.

Offset PLLs combine frequency mixing with frequency division in the feedback path to reduce the overall frequency multiplication factor inside the loop. The overall architecture is complicated by the use of DDS sources for frequency sweeping and the spuri generated by the DDS and the mixer have to be filtered. State-of-the-art DDS synthesisers have better phase noise than PLL synthesisers although they are costlier, and they suffer from spuri problems [33]. The DDS output usually needs to be frequency mixed to the desired frequency band, and mixers produce their own spuri.

Parasitic nonlinearities in the linear FMCW waveform due to, for example, nonlinear tuning curves of voltage controlled oscillators (VCO) also lead to spectral broadening but are considered systematic noise [37], [40]–[42] as opposed to phase noise that is random in nature. The influence of sweep linearity on FMCW radar system performance has been addressed in [37], [40]. A combination of VCOs and frequency multipliers is commonly used in FMCW radar systems to reduce the effects of the VCO's non-linear tuning characteristic [43].

B. Frequency Multipliers

Fig. 3a shows the propagation of phase noise through a frequency multiplier [31]. The timing jitter is preserved during the frequency multiplication process while the RMS phase noise increases by N , where N is the frequency multiplication factor. Frequency multipliers are used in conjunction with frequency synthesisers to increase the FM modulation index of the transmitted signal to combat VCO non-linearities [43]. It is well-known that the phase noise sidebands increase as $20 \log_{10} N$ dB under frequency multiplication (so that the *phase SNR* degrades by $20 \log_{10} N$ dB). However, it is important to note that this increase happens only when the small phase noise approximation is valid even after the frequency multiplication.

Special results have been derived for frequency multiplication of the type of spectrum shown in Fig. 1b. In [12], [24], [25] it has been demonstrated using theoretical analysis and practical measurements that if $\sigma_\phi^2 < 1$ then under frequency multiplication by N , W_p stays the same while L_p increases as $20 \log_{10}(N)$ as expected. However, when $\sigma_\phi^2 > 1$ the carrier starts broadening and so does the noise pedestal. For radar systems this phenomenon would result in the target response being broader so that it occupies a larger number of range bin, which is undesirable.

The carrier's 3-dB linewidth also increases under the process of frequency multiplication [14]. In general the linewidth increases N^2 -times if the radar signal has white frequency noise, N -times if it has flicker-frequency noise, and $N^{2/3}$ -times if it has random-walk frequency noise [12], [14]. However for short time delays, the phase noise processes decorrelate (explained shortly) which leads to a narrower linewidth than predicted [44].

C. Mixers

Fig. 3b shows the propagation of phase noise through a mixer [31]. Mixers can be used for up-conversion in the

transmitter (instead of frequency multipliers), and for down-conversion in the receiver. When implemented in the transmitter chain, the phase noise of the frequency synthesisers adds to that of the local oscillator. When implemented in the FMCW receiver chain, the inputs to the mixer are the transmitted and the received signals, while the output of the mixer is the IF signal. Mixers add or cancel the phase noise in the input signals: cancellation of phase noise happens when the two input signals are *coherent*, i.e. they have a defined phase relationship with each other (or in other words, are derived from the same reference source). It has been shown that in radar systems the mixing of the time-delayed transmitted signal with itself causes phase noise decorrelation as follows [4], [5], [45], [46]:

$$\mathcal{L}_{IF}(f) = \mathcal{L}_{Tx}(f) \times 4 \sin^2(\pi f \tau_d), \quad (10)$$

where τ_d is the round-trip time-delay to the target. This relationship will be analysed in detail later in this section. A caveat in (10) is on the usage of the offset frequency variable f . While the *operating frequency* at the IF can be orders of magnitude lower than the operating frequency at the Tx (i.e. the transmitter), the *offset frequency* f stays the same. In other words, (10) relates the phase noise at an offset f from the IF operating frequency to the phase noise at the same offset f at the transmitter's operating frequency.

Equation (10) implies that the integrated (RMS) phase noise at the IF stage in Fig. 2 is:

$$\sigma_{\phi_{IF}}^2 = \int_0^\infty 2\mathcal{L}_{Tx}(f) \times 4 \sin^2(\pi f \tau_d) df. \quad (11)$$

In general, for smaller τ_d the phase noise cancellation will be large. Correspondingly, $\sigma_{\phi_{IF}}^2$ will be small. The converse is true in general for large τ_d .

Referring to Fig. 3b, if the two inputs to the mixer are uncorrelated, the integrated output phase noise will be:

$$\sigma_{\phi_o}^2 = \sigma_{\phi_{i1}}^2 + \sigma_{\phi_{i2}}^2 = \omega_1^2 \sigma_{ti1}^2 + \omega_2^2 \sigma_{ti2}^2, \quad (12)$$

even for the difference frequency signal. If the two signals have *roughly* the same operating frequency and phase jitter we get,

$$\sigma_{\phi_o}^2 = \omega_o^2 \sigma_{to}^2 \approx 2\sigma_{\phi_i}^2 = 2\omega_i^2 \sigma_{ti}^2. \quad (13)$$

This situation happens in, for example, millimetre wave (MMW) FMCW radars where the two inputs to the mixer have almost the same operating frequency so that their difference frequency is a very low frequency IF signal. The above result shows that for incoherent inputs the IF signal's integrated phase noise is twice that of the transmitted signal: however the relationship for timing jitter is more interesting. Equation (13) can be rearranged as follows:

$$\sigma_{to}^2 \approx 2 \frac{\omega_i^2}{\omega_o^2} \sigma_{ti}^2, \quad (14)$$

or using the radar terminology,

$$\sigma_{t_{IF}}^2 \approx 2 \frac{\omega_{RF}^2}{\omega_{IF}^2} \sigma_{t_{RF}}^2, \quad (15)$$

which implies that the timing jitter in the IF signal is much larger than the timing jitter in the RF signal because generally $\omega_{RF} \gg \omega_{IF}$. This result will be used in the next subsection.

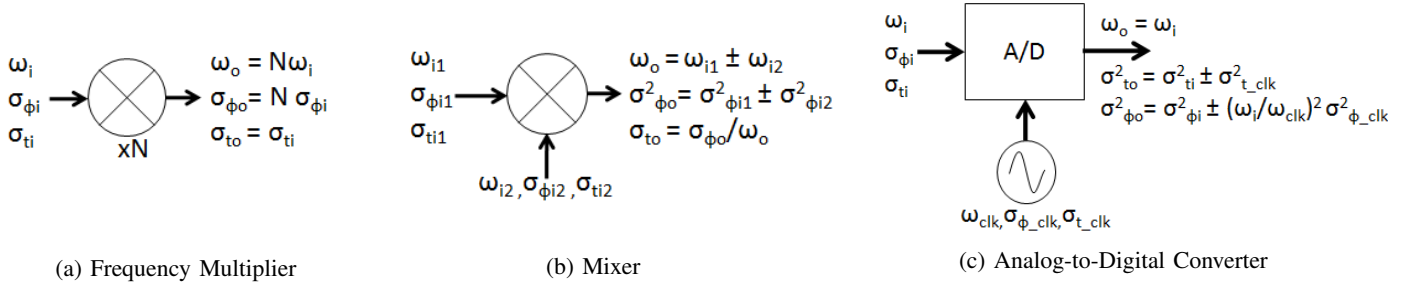


Fig. 3: Phase noise propagation through electronic subsystems.

D. Analog-to-Digital Converter

The subject of phase jitter/noise in ADCs has been dealt with in [47]–[52]. As shown in Fig. 3c, from the noise perspective the ADC can be thought of as a time-modulator or a time-mixer. Extending the argument of coherent phase noise cancellation in mixers, we propose that if the input signal is coherent with the sampling clock, the jitter in the sampled signal is *time-decorrelated* in the same way as the inputs to a mixer are *phase-decorrelated*. The decorrelation will be dependent on the time-delay between the signal being sampled and the clock signal, and most importantly how close the time jitters on the two are.

If the radar’s transmitted signal and the sampling clock are derived from the same reference source then their time jitters can be close to each other. However, as noted in (15) the IF signal being sampled has a time jitter greater than the received RF signal by a large factor. So the time jitter cancellation is less effective in this case. Nevertheless, as a guideline the transmitted signal’s phase jitter is related to the reference oscillator’s phase jitter through the transfer function of the frequency synthesiser being employed. For example, for a PLL synthesiser the *in-band* phase jitter at the output of the PLL is equal to the phase jitter in the reference oscillator, while beyond the loop bandwidth the phase jitter at the input and the output of the PLL are uncorrelated. In this case the ADC’s sampling clock can be used to partially cancel the in-band phase jitter (according to the time delay) while there will be no noise cancellation for frequency offsets outside the loop bandwidth.

For the non-coherent case, the jitter in the sampling clock adds to the jitter in the input signal. Therefore the integrated phase noise in the sampled signal is,

$$\sigma_{\phi o}^2 = \omega_o^2 \sigma_{t o}^2 = \omega_i^2 [\sigma_{t i}^2 + \sigma_{t_clk}^2] = \sigma_{\phi i}^2 + \frac{\omega_i^2}{\omega_{clk}^2} \sigma_{\phi_clk}^2. \quad (16)$$

Due to the term $\omega_i^2/\omega_{clk}^2$ a higher IF frequency input signal experiences a larger phase noise transferred from the sampling clock. A detailed analysis of (16) in the context of radars is presented in [52].

E. Phase noise decorrelation

The phase noise decorrelation factor in (10) is $4 \sin^2(\pi f \tau_d)$. This factor introduces periodic ripples in the demodulated phase noise spectrum as a function of τ_d . The critical value in (10) is the frequency offset of $f \tau_d = 1/6$ for which

$\mathcal{L}_{IF}(f) = \mathcal{L}_{Tx}(f)$. Beyond this frequency offset no further phase noise cancellation happens: in fact $\mathcal{L}_{Tx}(f)$ and $\mathcal{L}_{Rx}(f)$ add *in-phase* so that $\mathcal{L}_{IF}(f)$ starts increasing. The following points can be note:

- Coherent phase noise cancellation happens for frequency offsets $f \leq 1/6\tau_d$
- At $f\tau_d = 1/4$, $\mathcal{L}_{IF}(f) = 2\mathcal{L}_{Tx}(f)$.
- Finally for $f = 1/(2\tau_d)$, $\mathcal{L}_{IF}(f) = 4\mathcal{L}_{Tx}(f)$.

The last point implies that due to coherent mixing the resultant phase noise can be up to 6 dB larger than the transmitter’s phase noise.

The above discussion is valid for delay times less than the coherence time of the oscillator [14], [16]. As pointed out earlier, for excessively large measurement times (or measurements at very long ranges in the case of radar systems), the frequency noise processes in the oscillators cause excessive broadening of the measured RF spectrum [27]–[30]. An analysis of how the power shifts between the carrier portion and the sideband portion of the spectrum as a function of the delay time τ_d is given in [28], [44].

As a final comment, if non-coherent frequency mixing is used in a radar system, no cancellation of phase noise will happen at any range. In fact, the IF phase noise will just be twice the transmitter’s phase noise and no coherent ripples will be observed. The linewidth of target response will also be larger compared with a coherent radar.

F. System Noise Floor

Fig. 2 shows two amplifiers in the system that affect the noise floor performance of the overall system [5], [17]. Including a low-noise amplifier (LNA) as the first stage in the receiver minimises the thermal noise floor of the system. However, there are two major drawbacks of using an LNA. Firstly, targets close to the radar cause large reflected signals. The LNA further amplifies these signals causing the mixer stage to saturate earlier than when no LNA is present. Secondly, the direct leakage signal from the transmitter to the receiver is amplified further by the LNA. In some cases, this phase noise leakage signal can dominate the noise floor of the receiver, so that the thermal noise reduction of the LNA is negated. A power amplifier (PA) in the transmitter gives the radar the ability to detect further in range, but also increases the leakage signal. The PA can also distort the noise spectrum by adding an independent noise component (that will not be cancelled by the mixer), and also through AM noise to FM

noise conversion, which can be potentially significant when high levels of cancellation are required.

Therefore, a complete noise analysis needs to be done to compare the thermal noise floor to the leakage phase noise floor. Another path of phase noise leakage is through the receiver's mixer stage. Detailed analyses of these noise components can be found in [4], [5]. The additional noise from the PA can be dealt with by either taking the mixer LO from after the PA, or an additional leakage noise cancellation stage, as employed in some monostatic FMCW configurations.

As a final comment, it should be noted that the leakage signals demodulate to zero, or almost zero, operating frequency. Therefore, for the single-channel system shown in Fig. 2, the negative phase noise sideband will fold over and add to the positive sideband. Therefore, the average noise floor will be 3 dB higher. This, however, will not be a problem in a system utilising I/Q demodulation.

IV. THE MAXIMUM BOUND ON THE PEDESTAL HEIGHT L_p

Having discussed the troubles $\sigma_\phi^2 > 1$ can cause it is imperative to analyse this condition further for typical radar signal sources. Fig. 1b shows the phase noise pedestal in the RF spectrum centred at the carrier frequency ν_0 , along with the central carrier peak. A double-sided baseband model for the phase noise pedestal is the generalised Lorentzian function described in (7) but repeated here for convenience,

$$S_{RF}^p(f) = \frac{2L_p}{1 + \left[\frac{|f|}{0.5W_p} \right]^k}, \quad (17)$$

where L_p and W_p are indicated in Fig. 1b, and k is the order of the roll-off of the pedestal.

We will now derive the maximum bound on L_p for a given W_p in order to meet the condition $\sigma_\phi^2 < 1$ for $k \geq 2$. Note that the noise pedestal obviously does not include the central carrier peak and the phase noise floor. If $\sigma_\phi^2 < 1$ then σ_ϕ^2 is approximately equal to the RMS noise power in the pedestal and can be computed as:

$$\sigma_\phi^2 = \int_0^\infty S_{RF}^p(f) df. \quad (18)$$

The above integral was solved for various values of k : the results are shown in Table I. The second column shows that the integral converges to $\sigma_\phi^2 = W_p L_p$ in the limit of large k . The third column shows the maximum bound for L_p as a function of W_p for each k .

Also shown in Table I (fourth column) are computed L_p 's for $W_p/2 = 100$ kHz (this value of W_p is used in the plots in the next section). Note that 3 dB is to be subtracted from the value of L_p in dB-rad²/Hz to compute the single-sideband level of L_p in dBc/Hz: the latter will be the representative value for L_p measured on a spectrum analyser centred at the carrier frequency ν_0 .

Table I shows an interesting result that the maximum bound on L_p does not change significantly with k . The maximum value of the integral is at $k = 2$ and gives the tightest bound on L_p . Therefore, to ensure $\sigma_\phi^2 < 1$ we need,

$$L_p < \frac{2}{\pi W_p}. \quad (19)$$

TABLE I: Maximum allowable L_p for various values of k .

k	σ_ϕ^2 (rad ²)	Max L_p (rad ² /Hz)	Max L_p for $W_p = 200$ kHz
2	$\frac{\pi}{2} W_p L_p$	$0.64/W_p$	-58 dBc/Hz
2.5	$1.32 W_p L_p$	$0.76/W_p$	-57.2 dBc/Hz
3	$1.12 W_p L_p$	$0.89/W_p$	-56.5 dBc/Hz
4	$1.11 W_p L_p$	$0.9/W_p$	-56.5 dBc/Hz
12	$1.01 W_p L_p$	$0.99/W_p$	-56.1 dBc/Hz

TABLE II: Parameters of the FMCW radar being studied.

Parameters	MMW Radar
Carrier Frequency, ν_0	76.5 GHz
Swept Bandwidth, B_S	660 MHz
Sweep Time, T_S	1.25 ms
FFT Bandwidth, $1/T_S$	800 Hz
Freq. Multiplication Factor, N	8
PLL Loop Bandwidth, B_L	100 kHz
PLL In-band noise level, L_p	-88 dBc/Hz
Window Function	Blackman-Harris

The beauty of (19) is that this result does not depend on the actual operating frequency of the radar or the multiplication factor. The radar's transmitter only needs to comply with this limit as a minimum to be an acceptable radar signal source. If L_p and W_p are even lower, the radar signal source will remain coherent with itself (or *self-coherent*) to a much larger range than a radar signal source having larger L_p and W_p . The model developed here closely agrees with the measurements in [12] which also happen to be at 9.5 GHz.

A change in W_p would directly affect the bound on L_p . For example, if a noise bandwidth of 10 kHz was sufficient for the PLL employed in the transmitter then $W_p = 20$ kHz and the maximum allowable $L_p = -48$ dBc/Hz to ensure $\sigma_\phi^2 < 1$. Therefore, by reducing W_p the bound on L_p has been relaxed. Finally we emphasise that the bound on L_p has been stated in the units of dBc/Hz (i.e. normalised to the integration bandwidth) and should be used as such.

V. APPLICATION OF PHASE NOISE MODELLING TO A MMW FMCW RADAR SYSTEM

The phase noise modelling methodology was applied to a commercial MMW FMCW radar system having subsystems as in Fig. 2. The parameters of the radar system are shown in Table II. First, a PLL-based radar signal source will be used to measure the target responses of trihedral corner reflectors. The phase noise sidebands will be visible in this measurement. Next a low phase noise source will be used for the same measurement to demonstrate the performance improvement.

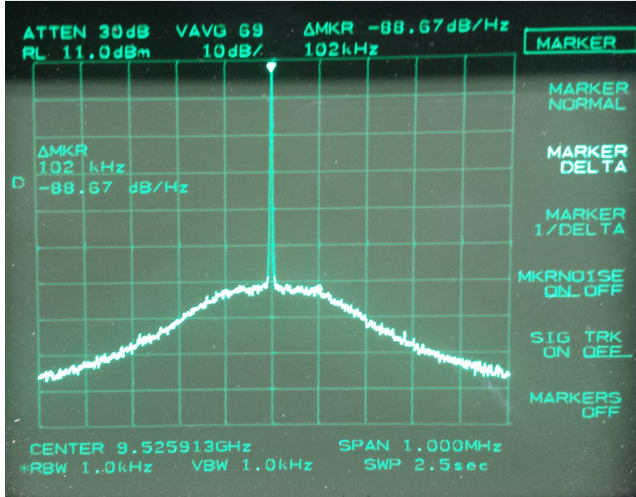


Fig. 4: Measured RF Spectrum of an X-band PLL synthesised oscillator.

A. Phase Noise Modelling of the PLL Based System

The radar used for measurements initially employed a PLL/VCO scheme to generate the X-band signal that was frequency multiplied to 76.5 GHz. Fig. 4 show a spectrum analyser display of the non-sweeping carrier signal. Since the swept bandwidth is small compared with the carrier, the same phase noise levels will be expected for the swept signal. The phase noise sidebands are visible: for example, at 100 kHz the phase noise is around -88 dBc/Hz.

A spectrum measurement of the transmitted signal at 76.5 GHz was also done (but not included here) which confirmed that there was no change in the width of the noise pedestal, and the pedestal height did go up by $20 \log N = 18$ dB. This conforms to the theory presented in the last section: the noise pedestal height $L_p = -88$ dBc/Hz is much less than the maximum bound suggested by Table I. Fig. 5 shows the final simulated single sideband target response at various target ranges taking into account the effects of phase noise decorrelation using (10). This type of simulation model is extremely useful in predicting the expected target response to analyse the phase noise performance of radar systems. The simulated target response is 6 dB higher at the peak of the coherent ripples as expected. The critical frequency offset $f_{crit} = 1/6\tau_d$ (converted to range bin values) is plotted as a vertical dotted line: it can be seen that beyond this point the phase noise sideband increases up to 6 dB beyond the transmitter's integrated phase noise level, and there is no further phase noise cancellation other than the troughs of the ripples.

The simulated target response at 150 m has a peak phase noise level of -45 dBc, while the simulated target response at 750 m has a peak phase noise level of -33 dBc. These values are to be compared with the measurement results of the next subsection. Due to the large difference between the RF operating frequency (76.5 GHz) and the IF (up to 7 MHz) the computed effect of the ADC jitter was minimal, and had minimal effect on the measurements.

B. Measurement results from the PLL based radar

Fig. 6 displays a measurement on two corner reflector targets placed at 173 m and 770 m respectively. The measurements were done using a CTS Radar system developed by Navtech Radar Ltd. having the parameters displayed in Table II. This figure also appears in [9] but has been subject to new analysis. It can be seen that thermal noise is superimposed on the phase noise sidebands, so the average noise level should be taken as the representative value of phase noise. The lower end of the two double-arrows have been placed to indicate the expected signal to phase noise level.

Comparing with Fig. 5 it can be seen that the theoretical modelling is compatible with the experimental results. The measured target response at 173 m indeed has an average phase noise level of around -45 dBc, while the measured target response at 770 m has an average phase noise level of around -33 dBc.

C. Discussion on the measurements from the PLL based radar

The modulation loop bandwidth of 100 kHz causes the PLL to have a large noise bandwidth (or noise pedestal width) of 200 kHz. The upshot is that both targets in Fig. 6 have large shoulder-like sidebands superimposed on them. This phenomenon causes severe difficulties in the detection and tracking of the objects in the region having a raised noise floor: the detection of all targets is degraded and small target can disappear in this noise floor.

To gain a better understanding of the artefacts of phase noise, we used a higher power radar with 17.5 cm range bins. Fig. 7 displays the measured target response of the 770 m corner reflector. Averaging was turned on to reduce the variance of the noise components in the display. The coherent sideband structure is much more visible in this plot along with other small targets (grass at shorter-ranges and trees at longer ranges). The coherent ripples can be compared with the top-right inset in Fig. 5. It can be noticed that the measured sideband level is now at -30 dBc instead of -33 dBc because this particular radar uses a tighter loop bandwidth, causing an increase in the in-band phase noise. However this does not affect the width of the coherent ripples.

It is worth noting that the coherent ripples in Fig. 7 were only visible after the *systematic noise* was mitigated in the frequency synthesiser [32]. The presence of systematic noises can smear the sideband structure and also cause a raised noise floor. We will not dwell further on systematic noise.

D. Improved phase noise design

To lower the phase noise sidebands we designed a low-phase noise frequency synthesiser. A spectrum analyser display of the synthesiser's output is shown in Fig. 8. A comparison with Fig. 4 shows that the new synthesiser indeed has very low phase noise for a compact, low-cost source. At the 100 kHz offset the measured phase noise is -111.8 dBc/Hz which is at least 23 dB better than the PLL source (as this measurement is close to the spectrum analyser's noise floor): the actual improvement is greater than 30 dB as shown next. A comparison of the modelled phase noise spectra of the two

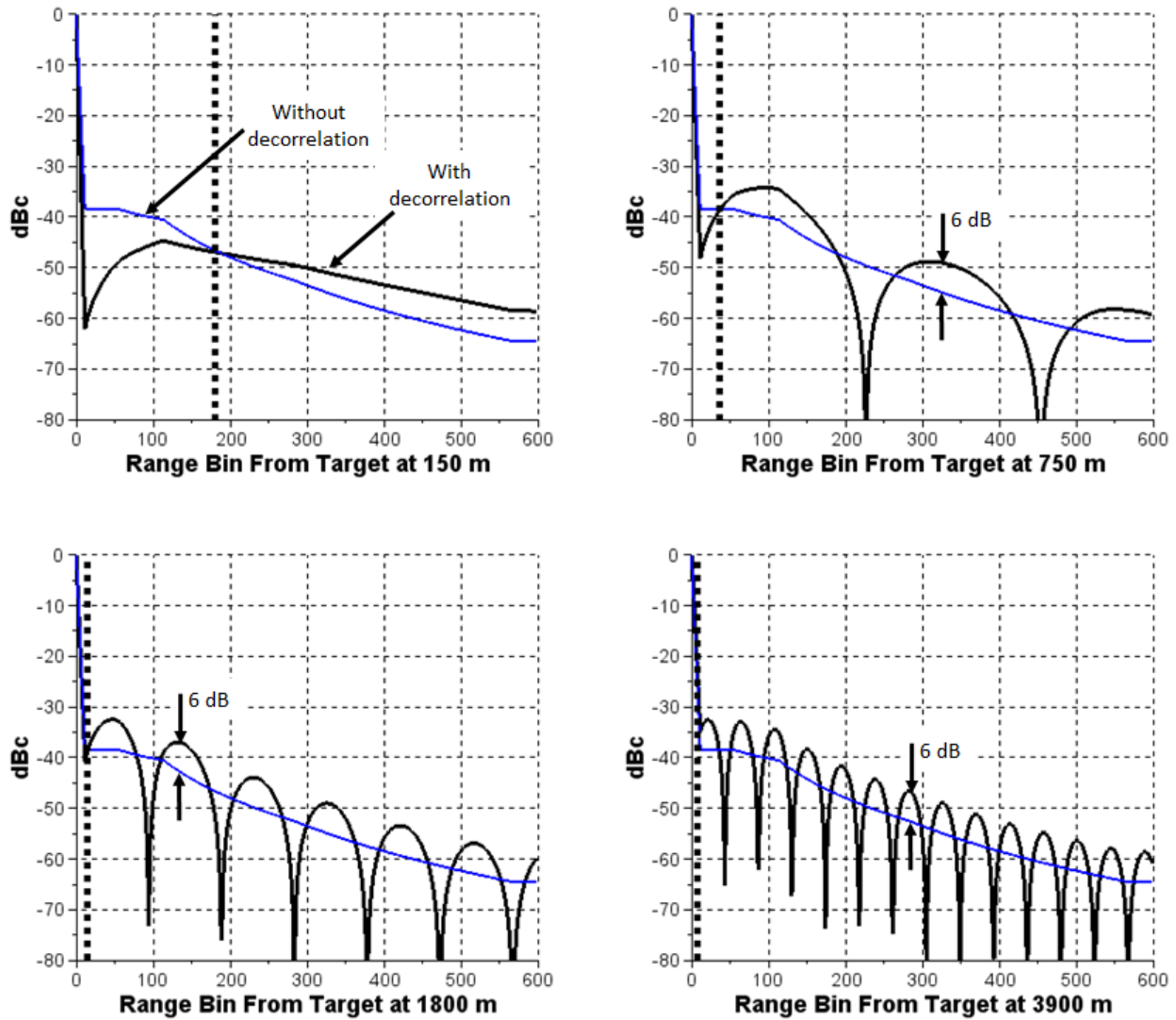


Fig. 5: Plots of the target response (single-sideband) at various ranges. Coherent phase noise cancellation gives an improvement (reduction) in phase noise in the region to the left of the vertical dotted line.

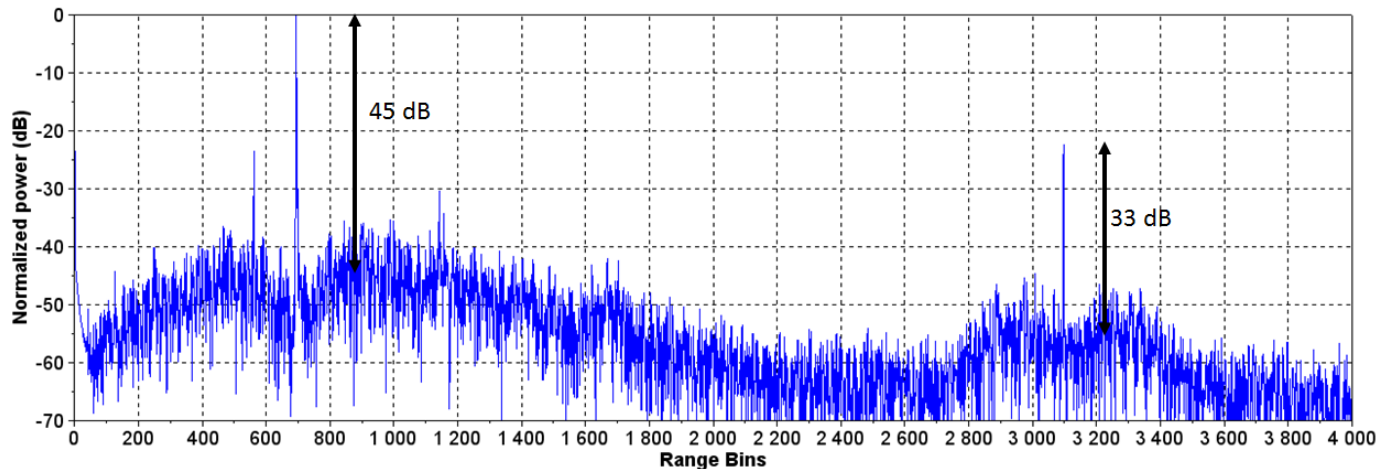


Fig. 6: Targets at 173m and 770m. Range bins are 25 cm each.

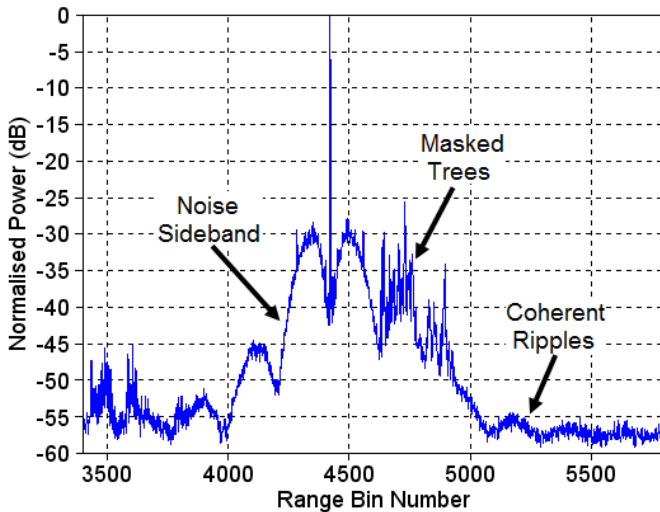


Fig. 7: The 770 m target's response produced by a higher power radar employing a PLL-based source.

sources is presented in Fig. 9. The huge improvement in the phase noise sidebands and the phase noise floor can be noticed. The effects of decorrelation in the new low-noise synthesiser can be worked out using plots similar to Fig. 5.

Fig. 10 shows the same scene as in Fig. 7, viewed with the higher-power radar system employing the new low-noise frequency synthesiser. A remarkable improvement in the phase noise sidebands of around 30 dB can be seen, significantly improving the definition in the scene. The grassy patch before the target and the trees after the target are clearly visible now. In addition, a hedge right behind the corner reflector has now been revealed that was completely hidden in Fig. 7. Therefore, any small targets near this large target can now be detected with precision. Potential applications of this type of improvement are in perimeter security systems where an intruder is walking right next to a large building: a conventional radar sensor will fail to pick up the intruder due to the spread of the phase noise sidebands around the building's large radar response. However an improved radar system based on low-phase noise technology will indeed be able to detect the intruder and raise an alarm.

VI. CONCLUSION

There are many causes of spectral broadening of the target responses in FMCW radar systems including internal factor like phase noise, unfocused lenses, and parasitic nonlinearities due to VCO tuning curves, and external factors like cross-demodulated radar interference signals [53], environmental precipitation, and distributed targets. This paper exclusively focused on the sideband spectral broadening of the radar target responses due to phase noise. A complete phase noise analysis methodology was described to model the phase noise at various stages of a complete radar system. New models of phase noise in ADCs and of phase noise pedestals were presented and applied to modelling phase noise in radar systems. Factors affecting the linewidth of the demodulated signal were discussed. Measurements were presented that are

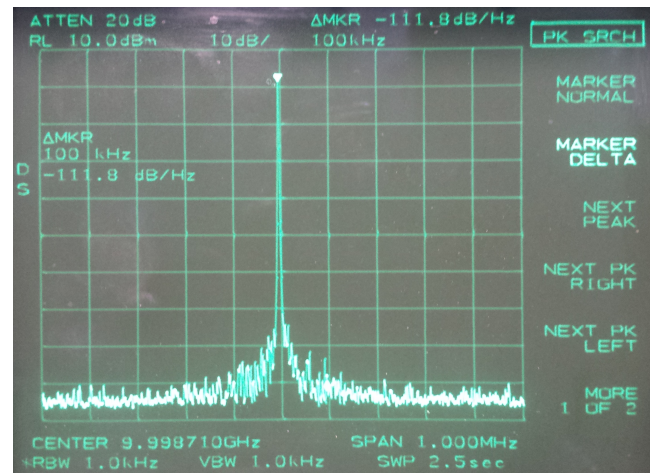


Fig. 8: Measured RF Spectrum of the low phase noise source.

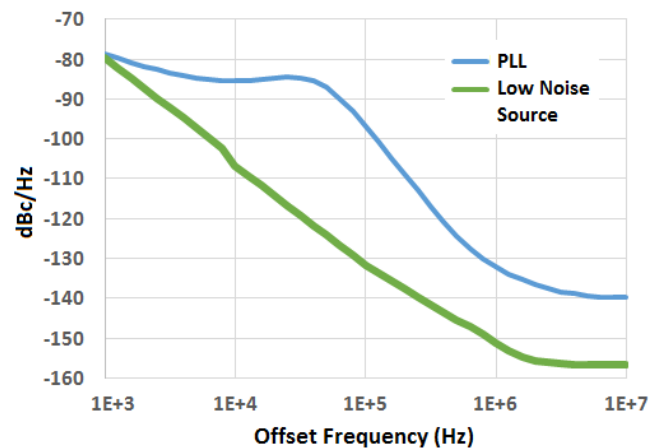


Fig. 9: Phase noise modelling of the PLL source and the low-noise source at 9.5 GHz.

in very good agreement with the developed theory. Finally, the use of a low-phase noise frequency synthesiser was described to reduce the phase noise sidebands by 30 dB, significantly improving the detection and tracking performance of the radar.

REFERENCES

- [1] A. Demir, A. Mehrotra, and J. Roychowdhury, "Phase noise in oscillators: a unifying theory and numerical methods for characterization," *IEEE Transactions on Circuits and Systems I: Fundamental Theory and Applications*, vol. 47, no. 5, pp. 655–674, May 2000.
- [2] A. Hajimiri and T. H. Lee, "A general theory of phase noise in electrical oscillators," *IEEE Journal of Solid-State Circuits*, vol. 33, no. 2, pp. 179–194, Feb 1998.
- [3] D. B. Leeson, "A simple model of feedback oscillator noise spectrum," *Proceedings of the IEEE*, vol. 54, no. 2, pp. 329–330, Feb 1966.
- [4] S. J. Goldman, *Phase Noise Analysis in Radar Systems Using Personal Computers*. Wiley-Interscience, 1989.
- [5] A. G. Stove, "Linear FMCW radar techniques," *IEE Proceedings F - Radar and Signal Processing*, vol. 139, no. 5, pp. 343–350, Oct 1992.
- [6] E. Baghdady, J. B. Nelin, and R. Lincoln, "Short-Term Frequency Stability: Characterization, Theory, and Measurement," *Proceedings of the IEEE*, 1965.
- [7] D. B. Leeson and G. F. Johnson, "Short-term stability for a doppler radar: Requirements, measurements, and techniques," *Proceedings of the IEEE*, vol. 54, no. 2, pp. 244–248, Feb 1966.
- [8] M. I. Skolnik, *Radar Handbook, 2nd Ed.* McGraw-Hill, 1990, pp. 15.48–15.50.

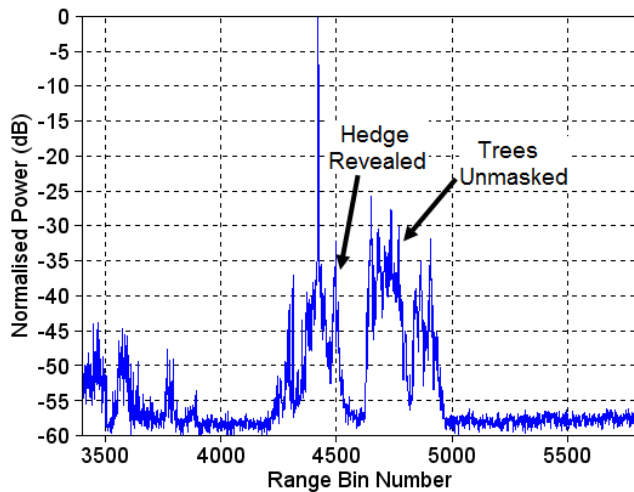


Fig. 10: The 770 m target displayed by a higher power radar with the low phase noise source. The phase noise sidebands have been largely eliminated.

- [9] K. Siddiq, R. J. Watson, S. R. Pennock, P. Avery, R. Poulton, and B. Dakin-Norris, "Phase noise analysis in FMCW radar systems," in *Radar Conference (EuRAD), 2015 European*, Sept 2015, pp. 501–504.
- [10] W. C. Lindsey and C. M. Chie, "Frequency Multiplication Effects on Oscillator Instability," *IEEE Transactions on Instrumentation and Measurement*, vol. IM-27, no. 1, 1978.
- [11] J. Rutman, "Characterization of Phase Frequency Instabilities in Precision Frequency Sources: Fifteen Years of Progress," *Proc IEEE*, vol. 66, no. 9, 1978.
- [12] F. L. Walls and A. DeMarchi, "RF Spectrum of a Signal after Frequency Multiplication: Measurement and Comparison with a Simple Calculation," *IEEE Transactions on Instrumentation and Measurement*, 1975.
- [13] X. Zhang, B. J. Rizzi, and J. Kramer, "A new measurement approach for phase noise at close-in offset frequencies of free-running oscillators," *IEEE Transactions on Microwave Theory and Techniques*, vol. 44, no. 12, pp. 2711–2717, Dec 1996.
- [14] D. Halford, "Infrared-Microwave Frequency Synthesis Design: Some Relevant Conceptual Noise Aspects," *Proc. Frequency Standard and Metrology Seminar*, Sep 1971.
- [15] A. Chorti and M. Brookes, "Resolving near-carrier spectral infinities due to $1/f$ phase noise in oscillators," in *2007 IEEE International Conference on Acoustics, Speech and Signal Processing - ICASSP '07*, vol. 3, April 2007, pp. III-1005–III-1008.
- [16] R. D. Weglein, "The Coherence of a Radar Master Oscillator," *40th Annual Frequency Control Symposium*, pp. 379–384, 1986.
- [17] P. D. L. Beasley, "The Influence of Transmitter Phase Noise on FMCW Radar Performance," in *2006 European Radar Conference*, Sept 2006, pp. 331–334.
- [18] M. Dudek, I. Nasr, D. Kissinger, R. Weigel, and G. Fischer, "The impact of phase noise parameters on target signal detection in FMCW-radar system simulations for automotive applications," in *Proceedings of 2011 IEEE CIE International Conference on Radar*, vol. 1, Oct 2011, pp. 494–497.
- [19] C. Baktir, E. Sobaci, and A. Dnmez, "A guide to reduce the phase noise effect in FMCW Radars," in *2012 IEEE Radar Conference*, May 2012, pp. 0236–0239.
- [20] M. E. Adamski, K. S. Kulpa, M. Nalecz, and A. Wojtkiewicz, "Phase noise in two-dimensional spectrum of video signal in FMCW homodyne radar," in *13th International Conference on Microwaves, Radar and Wireless Communications. MIKON - 2000. Conference Proceedings (IEEE Cat. No.00EX428)*, vol. 2, 2000, pp. 645–648 vol.2.
- [21] K. S. Kulpa, "Novel method of decreasing influence of phase noise on FMCW radar," in *2001 CIE International Conference on Radar Proceedings (Cat No.01TH8559)*, 2001, pp. 319–323.
- [22] —, "Focusing range image in VCO based FMCW radar," in *2003 Proceedings of the International Conference on Radar (IEEE Cat. No.03EX695)*, Sept 2003, pp. 235–238.
- [23] "IEEE Standard Definitions of Physical Quantities for Fundamental Frequency and Time Metrology - Random Instabilities," *IEEE Std 1139-1999*, 1999.
- [24] E. Schlecht and I. Mehdi, "Effects of local oscillator phase noise on submillimeter-wave spectrometer performance," in *2014 39th International Conference on Infrared, Millimeter, and Terahertz waves (IRMMW-THz)*, Sept 2014, pp. 1–2.
- [25] E. Bava, A. D. Marchi, and A. Godone, "Spectral Analysis of Synthesized Signals in the mm Wavelength Region," *IEEE Transactions on Instrumentation and Measurement*, vol. 26, no. 2, pp. 128–132, June 1977.
- [26] W. C. Lindsey and C. M. Chie, "Theory of oscillator instability based upon structure functions," *Proceedings of the IEEE*, vol. 64, no. 12, pp. 1652–1666, Dec 1976.
- [27] M. J. O'Mahony and I. D. Henning, "Semiconductor laser linewidth broadening due to $1/f$ carrier noise," *Electronics Letters*, vol. 19, no. 23, pp. 1000–1001, November 1983.
- [28] L. B. Mercer, " $1/f$ frequency noise effects on self-heterodyne linewidth measurements," *Journal of Lightwave Technology*, vol. 9, no. 4, pp. 485–493, Apr 1991.
- [29] B. Joss, L. G. Bernier, and F. Gardiol, "RF Spectrum of the Oscillator Signal Under Non-Stationary Phase Instabilities," in *40th Annual Symposium on Frequency Control*, 1986, May 1986, pp. 300–305.
- [30] K. Kikuchi and T. Okoshi, "Dependence of semiconductor laser linewidth on measurement time: evidence of predominance of $1/f$ noise," *Electronics Letters*, vol. 21, no. 22, pp. 1011–1012, Oct 1985.
- [31] F. M. Gardner, *Phase-Lock Techniques*. Wiley-Interscience, 2005.
- [32] V. Manassewitsch, *Frequency Synthesizers: Theory and Design*. Wiley-Interscience, 2005.
- [33] U. L. Rohde, *Microwave and Wireless Synthesizers: Theory and Design*. Wiley-Interscience, 1997.
- [34] M. Pichler, A. Stelzer, P. Gulden, C. Seisenberger, and M. Vossiek, "Phase-Error Measurement and Compensation in PLL Frequency Synthesizers for FMCW Sensors - II: Theory," *IEEE Transactions on Circuits and Systems I: Regular Papers*, vol. 54, no. 6, pp. 1224–1235, June 2007.
- [35] C. Wagner, R. Feger, A. Haderer, A. Fischer, A. Stelzer, and H. Jager, "A 77-GHz FMCW radar using a digital phase-locked synthesizer," in *2008 IEEE MTT-S International Microwave Symposium Digest*, June 2008, pp. 351–354.
- [36] F. Herzel, A. Ergintav, and Y. Sun, "Phase Noise Modeling for Integrated PLLs in FMCW Radar," *IEEE Transactions on Circuits and Systems II: Express Briefs*, vol. 60, no. 3, pp. 137–141, March 2013.
- [37] C. Wagner, A. Stelzer, and H. Jager, "Estimation of FMCW radar system performance using measurement data of a 77-GHz transmitter," in *2006 Asia-Pacific Microwave Conference*, Dec 2006, pp. 1701–1704.
- [38] M. Pichler, A. Stelzer, P. Gulden, C. Seisenberger, and M. Vossiek, "Phase-Error Measurement and Compensation in PLL Frequency Synthesizers for FMCW Sensors - I: Context and Application," *IEEE Transactions on Circuits and Systems I: Regular Papers*, vol. 54, no. 5, pp. 1006–1017, May 2007.
- [39] S. Scheiblhofer, M. Tremml, S. Schuster, R. Feger, and A. Stelzer, "A versatile FMCW radar system simulator for millimeter-wave applications," in *2008 European Radar Conference*, Oct 2008, pp. 447–450.
- [40] R. A. Habel, M. Pelletier, F. Chenier, M. Lecours, and G. Y. Delisle, "Design of a high resolution millimeter wave FM-CW radar," in *Proceedings of Canadian Conference on Electrical and Computer Engineering*, Sep 1993, pp. 51–54 vol.1.
- [41] M. Vossiek, P. Heide, M. Nalezinski, and V. Magori, "Novel FMCW radar system concept with adaptive compensation of phase errors," in *1996 26th European Microwave Conference*, vol. 1, Sept 1996, pp. 135–139.
- [42] A. Frischen, J. Hasch, and C. Waldschmidt, "FMCW ramp non-linearity effects and measurement technique for cooperative radar," in *2015 European Radar Conference (EuRAD)*, Sept 2015, pp. 509–512.
- [43] J. B. Hagen, *Radio-Frequency Electronics: Circuits and Applications*. Cambridge University Press, 2009.
- [44] L. Richter, H. Mandelberg, M. Kruger, and P. McGrath, "Linewidth determination from self-heterodyne measurements with subcoherence delay times," *IEEE Journal of Quantum Electronics*, vol. 22, no. 11, pp. 2070–2074, Nov 1986.
- [45] R. S. Raven, "Requirements on master oscillators for coherent radar," *Proceedings of the IEEE*, vol. 54, no. 2, pp. 237–243, Feb 1966.
- [46] M. K. Hobden, "77GHz FMCW Radar Head Design Study: A Survey of Monostatic and Bistatic Architectures," *E2V Technologies Tech. Report 2006/007*, Jan 2006.

- [47] V. J. Arkesteijn, E. A. M. Klumperink, and B. Nauta, "Jitter requirements of the sampling clock in software radio receivers," *IEEE Transactions on Circuits and Systems II: Express Briefs*, vol. 53, no. 2, pp. 90–94, Feb 2006.
- [48] T. N. Guo, "Unique Measurement and Modeling of Total Phase Noise in RF Receiver," *IEEE Transactions on Circuits and Systems II: Express Briefs*, vol. 60, no. 5, pp. 262–266, May 2013.
- [49] N. D. Dalt, M. Harteneck, C. Sandner, and A. Wiesbauer, "On the jitter requirements of the sampling clock for analog-to-digital converters," *IEEE Transactions on Circuits and Systems I: Fundamental Theory and Applications*, vol. 49, no. 9, pp. 1354–1360, Sep 2002.
- [50] B. Brannon, "Sampled systems and the effects of clock phase noise and jitter," *Analog Devices Appl. Note AN-756*.
- [51] P. Smith, "Little known characteristics of phase noise," *Analog Devices Appl. Note AN-741*, Aug 2004.
- [52] K. Siddiq, R. J. Watson, S. R. Pennock, P. Avery, R. Poulton, and S. Martins, "Analysis of sampling clock phase noise in homodyne FMCW radar systems," in *2016 IEEE Radar Conference (RadarConf)*, May 2016.
- [53] G. M. Brooker, "Mutual interference of millimeter-wave radar systems," *IEEE Transactions on Electromagnetic Compatibility*, vol. 49, no. 1, pp. 170–181, Feb 2007.



Kashif Siddiq received the B.Eng. and MS degrees in Electrical Engineering from the National University of Sciences & Technology, Pakistan, in 2004 and 2007 respectively. He received the Ph.D. degree in Electronic & Electrical Engineering from the University of Bath, UK, in 2017. He is currently working as a Senior Radar Systems Engineer at Navtech Radar Ltd., UK. In 2015 he jointly won the *Design Team of the Year Award* at the British Engineering Excellence Awards. In the same year he was nominated for the *Business Leader of the Future*

Award by Innovate UK. He also won a gold medal for the best undergraduate design project in B.Eng. in 2004. His research interests include FMCW radar systems engineering, low-phase noise RF circuit design, and radar signal processing.



Mervyn K. Hobden joined the Royal Air Force as an apprentice in August 1961 and spent 3 years at No 1 Radio School, RAF Locking. He left the RAF in 1975 and after 2 years at the Chronometer Section, Royal Greenwich Observatory, joined the staff of Marconi Avionics, where he became section leader of the STTE Group on the Foxhunter Radar Project. After a short spell at Microwave Associates in Dunstable, in 1982 he joined the Microwave Group of Marconi Electronics Devices Ltd in Lincoln as Principal Engineer. He became Chief Development

Engineer in 1986 and the Principal Systems Engineer with EEV when the military businesses were combined in 1995. In 2000 he moved to head up the Sensors Group at Dynex in Lincoln. In 2003, EEV purchased that group and he returned to being Principal Systems Engineer at E2V, which post he held till his retirement in 2010. He has a total of six patents in the field of millimetre wave engineering and is an Honorary Fellow of the British Horological Institute for his work as co-founder of the John Harrison Research Group, which has successfully investigated the theoretical ideas of the 18th C clockmaker John Harrison. A pendulum clock based on Harrison's ideas has been under test at the Royal Greenwich Observatory under the auspices of NPL for the last two years and has beaten all previous records for long term stability of a pendulum clock.



Steve R. Pennock has been a lecturer at the University of Bath for 33 years, and has over 125 publications. His research interests include modelling electromagnetic effects in devices and radio propagation, ultrawideband antennas, radar and communication systems, ground penetrating radar, microwave electrochemistry, distributed antenna schemes, cognitive self-configuring radio networks, ultrawideband partial discharge monitoring systems, 3D printing of microwave circuits and conductive ceramic mesh networks for wear monitoring.



Robert J. Watson (M96) received the B.Eng. and Ph.D. degrees in electronic engineering from the University of Essex, Colchester, U.K., in 1992 and 1996, respectively. He was a Senior Research Officer in the Departments of Mathematics and Electronic Systems Engineering at the University of Essex, from 1995 to 1998, where he was involved in number of propagation and weather radar projects. Since October 1998 he has been at the Department of Electronic and Electrical Engineering, University of Bath, Bath, U.K., where he is currently Associate

Professor. He has consulted widely for industry. His research interests include radio-propagation modelling, radio-frequency engineering and remote sensing systems. He was formerly the UK Commission F representative for the International Union of Radio Science (URSI) 2005-2010. He has been an Associate Editor of the American Geophysical Union's Radio Science journal since 2010.